Available online at www.sciencedirect.com

SCIENCE DIRECT®

Journal of Catalysis 239 (2006) 470–477

JOURNAL OF CATALYSIS

www.elsevier.com/locate/jcat

Support effect in dehydrogenation of propane in the presence of CO_2 over supported gallium oxide catalysts

Bingjun Xu, Bo Zheng, Weiming Hua *, Yinghong Yue *, Zi Gao

Department of Chemistry and Shanghai Key Laboratory of Molecular Catalysis and Innovative Materials, Fudan University, Shanghai 200433, PR China

Received 16 January 2006; revised 22 February 2006; accepted 23 February 2006

Abstract

Dehydrogenation of propane to propene in the absence or presence of CO_2 over different supported gallium oxide catalysts was investigated. Ga_2O_3/TiO_2, Ga_2O_3/Al_2O_3, and Ga_2O_3/ZrO_2 catalysts exhibited high activity, and Ga_2O_3/SiO_2 and Ga_2O_3/MgO were ineffective catalysts for the dehydrogenation of propane. The conversions of propane over Ga_2O_3/TiO_2, Ga_2O_3/Al_2O_3, and Ga_2O_3/ZrO_2 catalysts at 600 °C reached 23, 33, and 39%, respectively. The high dehydrogenation activities are connected with the abundant medium-strong acid sites on the catalyst surface. Carbon dioxide can promote the catalytic dehydrogenation activity of Ga_2O_3/TiO_2 but suppress those of Ga_2O_3/ZrO_2 and Ga_2O_3/Al_2O_3. The conversion of propane becomes 32, 26, and 30% in the presence of CO_2 over Ga_2O_3/TiO_2, Ga_2O_3/Al_2O_3, and Ga_2O_3/ZrO_2 catalysts, respectively. Results of pulse reaction and the H_2 and propane chemisorptions indicate that two contrary roles of CO_2 exist in the reaction: the positive role of removing dissociatively adsorbed H_2 on catalyst surface through the reverse water–gas shift reaction and the negative role of displacing the propane adsorbed on basic sites of catalyst. XPS studies show that the different behavior of the five supported Ga_2O_3 catalysts may be attributed to the different interactions between the support and the Ga_2O_3 species. The dehydrogenation reaction is suggested to proceed through a heterolytic dissociation reaction pathway.

Keywords: Supported gallium oxide catalyst; Propane; Dehydrogenation; Carbon dioxide; Reaction mechanism

1. Introduction

The catalytic dehydrogenation of propane to propene is of increasing importance due to the growing demand for propene, which is an important raw material in the production of polypropene, polyacrylonitrile, acrolein, and acrylic acid. Dehydrogenation of propane is an endothermic reaction; therefore, relatively high reaction temperatures are needed to obtain high propane yields. The high reaction temperatures favor thermal cracking reactions to form light alkanes and alkenes, leading to decreased product yield and increased catalyst deactivation. Catalytic oxidative dehydrogenation of propane by oxygen is an attractive alternative because it is an exothermic and non-thermodynamically limited reaction. However, the propene selectivity of the catalytic reaction remains an unsolved problem owing to the overoxidation of propane.

Recently, catalytic oxidative dehydrogenation of propane by carbon dioxide instead of oxygen has been attempted [1,2]. The promoting effect of carbon dioxide on the reaction has been observed on many catalysts, including silica-supported Cr_2O_3 [1,2], rare earth vanadates [3], and Ga_2O_3 [4]. Because carbon dioxide is one of the major greenhouse gases, the use of carbon dioxide is attractive not only economically, but also ecologically.

Aromatization of light paraffins over Ga-promoted HZSM-5 catalysts has been studied intensively in the last decade. The role of gallium oxide in the aromatization reaction is thought to facilitate the dehydrogenation steps, including the dehydrogenation of alkanes, higher olefins, and cycloolefins [5–10]. More recently, it has been found that carbon dioxide can markedly promote the dehydrogenation of ethane and propane over gallium oxide or supported gallium oxide catalysts [4,11–16]. But this promotional effect was not observed over all of the supported gallium oxide catalysts; in fact, the dehydrogenation reaction was sometimes inhibited, such as over

---

* Corresponding authors. Fax: +86 21 65641740.
E-mail address: yhyue@fudan.edu.cn (Y. Yue).

0021-9517/$ – see front matter © 2006 Elsevier Inc. All rights reserved.
doi:10.1016/j.jcat.2006.02.017

γ-Al_2O_3-supported Ga_2O_3 catalyst [12]. The reason for this unusual support effect remains still unclear. In addition, researchers have not yet reached agreement on the main role of carbon dioxide in reactions. Nakagawa et al. proposed CO_2-promoted desorption of olefin products from the catalyst surface [12], and Michorczyk et al. considered CO_2-consumed hydrogen via a reverse water–gas shift reaction [13]. In previous work we found that the reverse water–gas shift reaction and the Boudouard reaction of CO_2 may account for the enhanced catalytic activity and stability over Ga_2O_3 catalysts [16].

In the present work, five different supported gallium oxide catalysts Ga_2O_3/TiO_2, Ga_2O_3/Al_2O_3, Ga_2O_3/ZrO_2, Ga_2O_3/SiO_2, and Ga_2O_3/MgO were prepared and characterized. Their catalytic performance for dehydrogenation of propane to propene in the absence or presence of CO_2 was investigated, as was the support effect as well as the role of CO_2. Finally, a probable mechanism of the reaction over supported gallium oxide catalysts was proposed.

2. Experimental

2.1. Catalyst preparation

ZrO_2 and MgO were prepared by adding an aqueous solution of ammonia into $ZrOCl_2$ and $Mg(NO_3)_2$ solutions, respectively, followed by aging overnight, filtering, washing, drying, and calcining at 600 °C for 6 h. TiO_2 (Degussa P25), γ-Al_2O_3, and SiO_2 were purchased directly and used with no further treatment.

Supported gallium oxide catalysts containing 5 wt% Ga_2O_3 were prepared by impregnating an aqueous solution of $Ga(NO_3)_3 \cdot xH_2O$ (Aldrich) on TiO_2, γ-Al_2O_3, ZrO_2, SiO_2, or MgO using an incipient wetness method. The impregnated samples were dried at 100 °C and calcined at 600 °C for 6 h in air flow. The catalysts thus obtained were designated as Ga_2O_3/TiO_2, Ga_2O_3/Al_2O_3, Ga_2O_3/ZrO_2, Ga_2O_3/SiO_2, and Ga_2O_3/MgO.

2.2. Catalyst characterization

The specific surface areas of the catalysts were measured by nitrogen adsorption at −196 °C using a Micromeritics ASAP 2000 instrument and calculated by the BET method. Surface acidity was measured by NH_3 temperature-programmed desorption (NH_3-TPD) in a flow-type fixed-bed reactor at ambient pressure, and surface basicity was measured by CO_2 temperature-programmed desorption (CO_2-TPD) with a similar apparatus. A 100-mg sample was preheated at 600 °C for 3 h, and then cooled to 120 °C in flowing He. At this temperature, sufficient pulses of NH_3 or CO_2 were injected until adsorption saturation occurred, followed by purging with He for 2 h. The temperature was then raised from 120 to 600 °C at a rate of 10 °C/min, and the NH_3 or CO_2 desorbed was collected in a liquid N_2 trap and detected by on-line gas chromatography. Temperature-programmed reduction (TPR) experiments were carried out on a Micromeritics TPD/TPR 2900 instrument using 25 mg of catalyst under a mixed gas flow (40 ml/min) of hydrogen (10%) and argon (90%). The catalyst was pretreated in N_2 flow at 300 °C for 3 h. The temperature was increased from 50 to 600 °C at a ramp rate of 10 °C/min. A thermal conductivity detector (TCD) was used to monitor the hydrogen consumed during the TPR experiments. X-ray photoelectron spectroscopy (XPS) was performed using Al-K_α radiation (1486.6 eV) on a Perkin–Elmer PHI 5000C ESAC system with a base pressure of 1×10^{-9} Torr. The sample was pressed and degassed in the pretreatment chamber for 2 h before being transferred to the analysis chamber for XPS measurement. All binding energy (BE) values were referenced to the C 1s peak at 284.6 eV. H_2 and propane chemical adsorption measurements were carried out on a Micromeritics TPD/TPR 2900 instrument using 500 mg of catalyst under a argon gas flow (40 ml/min). The temperature was raised from room temperature to 600 °C at a rate of 10 °C/min, maintained at 600 °C for 2 h, and then cooled to the adsorption temperature (300 °C). For H_2 adsorption, several pulses of the mixed gas (10% hydrogen and 90% argon) with fixed volume were introduced until no more H_2 was adsorbed on the catalyst. For propane adsorption, when in the absence of CO_2, several pulses of propane with fixed volume were injected until no more propane was adsorbed on the catalyst. While in the presence of CO_2, the experiment conducted in the gas flow contained 5 vol% CO_2 and the balance argon instead of pure argon.

2.3. Reaction testing

Catalytic tests were performed in a fixed-bed flow microreactor at atmospheric pressure, with nitrogen as the carrier gas at a flow rate of 20 ml/min. The catalyst load was 200 mg, and it was activated at the reaction temperature (600 °C) for 1 h in nitrogen flow before the reaction. For dehydrogenation of propane in the absence of carbon dioxide, the gas reactant contained 2.5 vol% propane and the balance nitrogen. For the dehydrogenation of propane in the presence of carbon dioxide, the gas reactant contained 2.5 vol% propane, 5 vol% carbon dioxide, and the balance nitrogen.

The hydrocarbon reaction products were analyzed using an on-line gas chromatograph equipped with a 6-m packed column of Porapak Q and a flame ionization detector. The gas products, including N_2, CO, and CO_2, were analyzed on-line by another chromatograph equipped with a 2-m packed column of carbon molecular sieve 601 and a TCD. The conversion and selectivity were calculated as follows:

$$C_3H_8 \text{ conversion} = \frac{C_3H_{8\,\text{in}} - C_3H_{8\,\text{out}}}{C_3H_{8\,\text{in}}} \times 100\%,$$

$$CO_2 \text{ conversion} = \frac{CO_{2\,\text{in}} - CO_{2\,\text{out}}}{CO_{2\,\text{in}}} \times 100\%,$$

$$C_3H_6 \text{ selectivity} = \frac{C_3H_{6\,\text{out}}}{C_3H_{8\,\text{in}} - C_3H_{8\,\text{out}}} \times 100\%.$$

2.4. Pulse reaction

Pulse tests were carried out on a fixed-bed pulse microreactor. The catalyst load for the test was 200 mg. For CO_2 and

H_2 pulse testing, the catalyst was pretreated with He for 1 h at reaction temperature, after which a pulse of CO_2 and H_2 gas mixture (1:1 molar ratio; 2.0 ml) was injected. For CO_2 pulse reaction, the catalyst was first pretreated at the reaction temperature (600 °C) in He for 1 h and then in H_2 for 30 min; then He was used to purge the pulse reaction system for 10 min to remove H_2. Finally, a pulse of CO_2 (2.0 ml) was injected. He, at a flow rate of 20 ml/min, was used as the carrier gas.

The products of the pulse reaction were analyzed using an on-line gas chromatograph equipped with a 2-m packed column of carbon molecular sieve 601 and a TCD. The reaction data in the work were reproducible with a precision of $<5\%$.

3. Results

3.1. Catalyst characterization

TiO_2-, γ-Al_2O_3-, ZrO_2-, SiO_2-, and MgO-supported gallium oxide catalysts containing 5 wt% Ga_2O_3 were prepared by an incipient wetness method. Their powder X-ray diffraction patterns were measured. No other diffraction peaks but those of the supports were observed, indicating that gallium oxide was well dispersed on all of the supports. TPR experiments were also carried out to study the reducibility of these catalysts. No reduction peaks could be identified in the TPR profiles, suggesting that the supported gallium oxide catalysts cannot be reduced by hydrogen below 600 °C.

The surface acidity of the supported gallium oxide catalysts was measured by NH_3-TPD; the results are given in Table 1, together with those of the supports for comparison. All of the supports exhibited only one broad peak on the TPD profiles, in the range of 228–327 °C, indicating that the acid sites of the supports are of weak to medium strength. The acidity of the supports was modified significantly after being impregnated with gallium oxide. Evidently there were two desorption peaks on the TPD profiles of all of the supported gallium oxide catalysts. The low temperature peaks at about 218–313 °C and the high peaks at 392–442 °C corresponded to the weak and strong acid sites of the samples. The low temperature peaks were similar to those of the supports; therefore the emergence of the high temperature peaks can be attributed to the introduction of gallium oxide on the supports. Meanwhile, the impregnation of gallium oxide on the supports also significantly increased the total amount of surface acid sites, especially those of medium-strong acid strength (expressed as the amount of NH_3 desorbed at 350–600 °C), which are suggested to be active for the dehydrogenation reaction [16]. The amount of medium to strong acid sites of the catalysts has the following sequence: $Ga_2O_3/ZrO_2 > Ga_2O_3/Al_2O_3 > Ga_2O_3/TiO_2 > Ga_2O_3/SiO_2 > Ga_2O_3/MgO$.

The surface basicity of the supports and the supported gallium oxide catalysts were measured by CO_2-TPD. One broad CO_2 desorption peak was observed for all of the supports as well as the supported gallium oxide catalysts; the peak temperature and amount of desorbed CO_2 of all samples are summarized in Table 2. There was a much smaller number of basic sites than of acidic sites on all of the supported gallium oxide catalysts except for Ga_2O_3/MgO, possibly due to the relatively strong basic property of the MgO support. Therefore, the supported gallium oxides except Ga_2O_3/MgO are primarily acid catalysts. The sequence of increasing amount of basic sites on the catalyst surface was $Ga_2O_3/MgO > Ga_2O_3/ZrO_2 > Ga_2O_3/\gamma\text{-}Al_2O_3 > Ga_2O_3/TiO_2 \gg Ga_2O_3/SiO_2$.

The XPS spectra of supported gallium oxide catalysts were recorded. The deconvoluted spectra in the Ga 3d region are shown in Fig. 1. Only two peaks appear in the spectra of the Ga_2O_3/ZrO_2 and Ga_2O_3/Al_2O_3 catalysts, at about 24 and 21 eV, respectively, which can be assigned to O 2s and Ga^{3+} 3d bands according to the literature [17]. The Ga 3d banding energy was increased when gallium oxide was supported on ZrO_2 or Al_2O_3, indicating a strong interaction between the Ga_2O_3 species and the ZrO_2 or Al_2O_3 support, in accordance with previously reported results [18,19]. A low-energy peak (LBE) at 19.6 eV appeared in the spectrum of Ga_2O_3/TiO_2, Ga_2O_3/SiO_2, and Ga_2O_3/MgO catalysts, which can be attributed to the presence of $Ga^{\delta+}$ species ($\delta < 2$) [20], suggesting that Ga_2O_3 was partially reduced on these supports. Similar results have been reported previously [21], and the decrease of Ga 3d binding energy of the gallium species in the Ga_2O_3/TiO_2 catalyst has been tentatively attributed to desorption of some loosely bound surface oxygen atoms at high calcination temperatures. The relative ratios of the Ga^{3+} and $Ga^{\delta+}$ species of the three catalysts were calculated and the percentage of $Ga^{\delta+}$

Table 1
NH_3-TPD data of the supports and the supported gallium oxide catalysts

Catalyst	Peak temperature (°C)		Amount of desorbed NH_3 (mmol/g)		
	I	II	I (120–350 °C)	II (350–600 °C)	Total
Ga_2O_3/TiO_2	220	442	0.20	0.21	0.41
TiO_2	228	–[a]	0.18	0.12	0.30
Ga_2O_3/Al_2O_3	313	418	0.29	0.28	0.57
Al_2O_3	327	–[a]	0.22	0.19	0.41
Ga_2O_3/ZrO_2	310	436	0.37	0.34	0.71
ZrO_2	320	–[a]	0.16	0.24	0.40
Ga_2O_3/SiO_2	218	408	0.16	0.10	0.26
SiO_2	232	–[a]	0.07	0.06	0.13
Ga_2O_3/MgO	310	392	0.12	0.08	0.20
MgO	302	–[a]	0.06	0.02	0.08

[a] Not detected.

Table 2
CO_2-TPD data of the supports and the supported gallium oxide catalysts

Catalyst	Peak temperature (°C)	Amount of desorbed CO_2 (mmol/g)		
		I (120–350 °C)	II (350–600 °C)	Total
Ga_2O_3/TiO_2	250	0.06	0.02	0.08
TiO_2	222	0.05	0.01	0.06
Ga_2O_3/Al_2O_3	235	0.07	0.02	0.09
Al_2O_3	219	0.06	0.01	0.07
Ga_2O_3/ZrO_2	361	0.07	0.03	0.10
ZrO_2	320	0.06	0.02	0.08
Ga_2O_3/SiO_2	214	0.02	0	0.02
SiO_2	211	0.01	0	0.01
Ga_2O_3/MgO	293	0.13	0.06	0.19
MgO	302	0.12	0.06	0.18

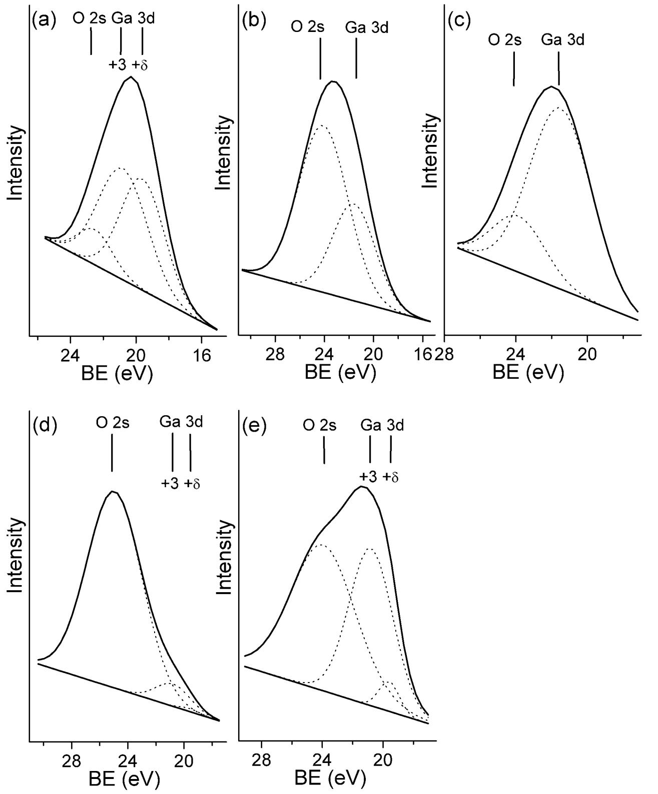

Fig. 1. XPS spectra of supported gallium oxide catalysts (Ga 3d) on (a) Ga_2O_3/TiO_2; (b) Ga_2O_3/Al_2O_3; (c) Ga_2O_3/ZrO_2; (d) Ga_2O_3/SiO_2; (e) Ga_2O_3/MgO.

Table 3
XPS data of supported gallium oxide catalysts

Catalyst	Ga 3d binding energy (eV)	Ga^{3+} (%)	$Ga^{\delta+}$ (%)[a]
β-Ga_2O_3	20.8 [16]	100	0
Ga_2O_3/TiO_2	19.6/20.8	55	45
Ga_2O_3/Al_2O_3	21.6	100	0
Ga_2O_3/ZrO_2	21.6	100	0
Ga_2O_3/SiO_2	19.6/20.8	93	7
Ga_2O_3/MgO	19.6/20.8	92	8

[a] $\delta < 2$.

species was found to decrease in the order $Ga_2O_3/TiO_2 \gg Ga_2O_3/MgO \approx Ga_2O_3/SiO_2$. The XPS results are summarized in Table 3.

3.2. Catalytic activity

Dehydrogenation of propane over supported gallium oxide catalysts in the absence of CO_2 was carried out at 600 °C; the results, along with the BET surface areas of the catalysts, are given in Table 4 and Fig. 2. The major product formed in the reaction was propene, and the minor products were methane, ethane, and ethylene. As Fig. 2 clearly shows, the catalytic behaviors of the five supported gallium oxide catalysts in the reaction differ considerably. The initial conversion of propane on the catalysts decreases in the order $Ga_2O_3/ZrO_2 > Ga_2O_3/Al_2O_3 > Ga_2O_3/TiO_2 > Ga_2O_3/SiO_2 > Ga_2O_3/MgO$, paralleling the sequence of the amount of medium to strong acid sites and indicating that surface acidity should play an important role in dehydrogenation. For all catalysts, propane conversion decreased along with the reaction time, but the decrease was much slower on the Ga_2O_3/Al_2O_3, Ga_2O_3/MgO, and Ga_2O_3/SiO_2 catalysts than on the Ga_2O_3/TiO_2 and Ga_2O_3/ZrO_2 catalysts. Catalyst deactivation is commonly attributed to the formation of coke on the catalyst surface.

Table 4
Reaction data in the absence of CO_2

Catalyst	S_{BET} (m^2/g)	Propane conversion (%)[a]	Selectivity (%)			
			CH_4	C_2H_4	C_2H_6	C_3H_6
Ga_2O_3/TiO_2	47	23	6.8	7.1	1.0	85
Ga_2O_3/Al_2O_3	102	33	3.2	4.2	0.8	92
Ga_2O_3/ZrO_2	19	39	9.1	13.2	3.6	74
Ga_2O_3/SiO_2	329	7.2	2.9	4.8	0.4	92
Ga_2O_3/MgO	35	5.3	11	33	22	34

[a] Reaction time: 10 min.

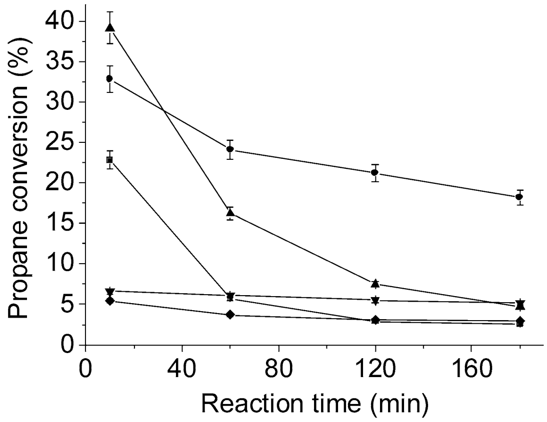

Fig. 2. Conversion of propane over supported gallium oxide catalysts in the absence of carbon dioxide: (■) Ga_2O_3/TiO_2; (●) Ga_2O_3/Al_2O_3; (▲) Ga_2O_3/ZrO_2; (▼) Ga_2O_3/SiO_2; (◆) Ga_2O_3/MgO.

Table 5
Reaction data in the presence of CO_2

Catalyst	Conversion (%)[a]		Selectivity (%)			
	C_3H_8	CO_2	CH_4	C_2H_4	C_2H_6	C_3H_6
Ga_2O_3/TiO_2	32	30	10	16	1.1	73
Ga_2O_3/Al_2O_3	26	5.2	2.9	3.8	0.4	94
Ga_2O_3/ZrO_2	30	29	14	17	4.2	65
Ga_2O_3/SiO_2	6.4	3.1	3.1	4.8	0.3	92
Ga_2O_3/MgO	4.3	4.2	10	33	28	29

[a] Reaction time: 10 min.

The dehydrogenation of propane was also run over the supported gallium oxide catalysts in the presence of CO_2 at 600 °C; the reaction data are summarized in Table 5 and Fig. 3. CO was detected in the reaction product. The addition of CO_2 in the dehydrogenation reaction has different effects on the Ga_2O_3/TiO_2, Ga_2O_3/Al_2O_3, Ga_2O_3/ZrO_2, Ga_2O_3/SiO_2, and Ga_2O_3/MgO catalysts. The initial activity of Ga_2O_3/TiO_2 in the presence of CO_2 was much higher than that in the absence of CO_2; in contrast, that of Ga_2O_3/Al_2O_3 and Ga_2O_3/ZrO_2

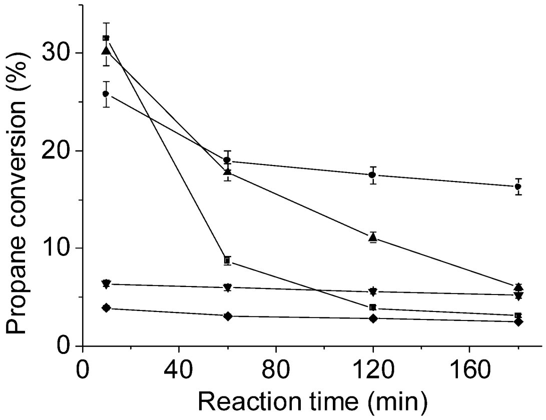

Fig. 3. Conversion of propane over supported gallium oxide catalysts in the presence of carbon dioxide: (■) Ga_2O_3/TiO_2; (●) Ga_2O_3/Al_2O_3; (▲) Ga_2O_3/ZrO_2; (▼) Ga_2O_3/SiO_2; (◆) Ga_2O_3/MgO.

Table 6
The conversion of CO_2 in reactions (1) and (2)[a]

Catalyst	$C_{(1)}$ (%)	$C_{(2)}$ (%)
Ga_2O_3/TiO_2	20	10
Ga_2O_3/Al_2O_3	2.1	3.1
Ga_2O_3/ZrO_2	2.9	26
Ga_2O_3/SiO_2	1.1	2.0
Ga_2O_3/MgO	1.1	3.1

[a] Reaction time: 10 min.

was reduced in the presence of CO_2, whereas for Ga_2O_3/MgO and Ga_2O_3/SiO_2, CO_2 seemed to have little effect on initial dehydrogenation activity. The initial conversion of propane on the catalysts in the presence of CO_2 decreased in the following order: $Ga_2O_3/TiO_2 > Ga_2O_3/ZrO_2 > Ga_2O_3/Al_2O_3 > Ga_2O_3/SiO_2 > Ga_2O_3/MgO$.

The amount of initial CO_2 conversion on the catalysts was in the order $Ga_2O_3/TiO_2 \approx Ga_2O_3/ZrO_2 \gg Ga_2O_3/Al_2O_3 \approx Ga_2O_3/SiO_2 \approx Ga_2O_3/MgO$, indicating that evidently CO_2 participated in dehydrogenation only over Ga_2O_3/TiO_2 and Ga_2O_3/ZrO_2. It has been reported that the dehydrogenation reaction can be influenced by CO_2 through the reverse water–gas shift reaction and the Boudouard reaction [16], as follows:

$$CO_2 + H_2 \rightarrow CO + H_2O \tag{1}$$

and

$$CO_2 + C \rightarrow 2CO. \tag{2}$$

The conversion of CO_2 in reactions (1) and (2) can be estimated from the amount of CO and CO_2 before and after the reaction, as follows:

$$C_{(2)} = \frac{n(CO_2)_{\text{after}} + n(CO) - n(CO_2)_{\text{before}}}{n(CO_2)_{\text{before}}} \times 100\%$$

and

$$C_{(1)} = C_{CO_2} - C_{(2)},$$

where $n(CO_2)_{\text{before}}$, $n(CO_2)_{\text{after}}$, $n(CO)$, and C_{CO_2} denote the amount of CO_2 before reaction, the amount of CO_2 after reaction, the amount of CO formed, and the conversion of CO_2, respectively. The results, given in Table 6, indicate that the effect of adding CO_2 differs among the five catalysts. For Ga_2O_3/TiO_2, CO_2 is consumed mainly through the reverse water–gas shift reaction, which may account for the enhancement of the dehydrogenation activity; whereas for Ga_2O_3/ZrO_2, the main role of CO_2 becomes the elimination of coke by the Boudouard reaction, which may account for the enhancement of stability of Ga_2O_3/ZrO_2 catalyst after the addition of CO_2 (Figs. 2 and 3).

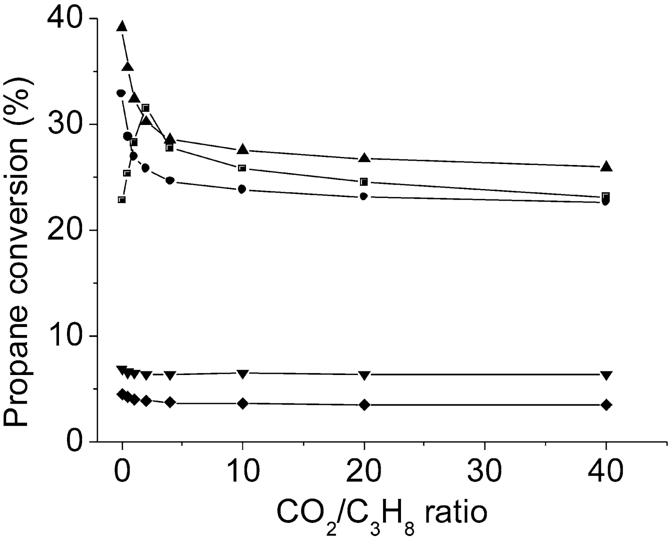

Fig. 4. Conversion of propane over supported gallium oxide catalysts with different CO_2/C_3H_8 ratios: (■) Ga_2O_3/TiO_2; (●) Ga_2O_3/Al_2O_3; (▲) Ga_2O_3/ZrO_2; (▼) Ga_2O_3/SiO_2; (◆) Ga_2O_3/MgO.

3.3. *Effect of the CO_2/C_3H_8 ratio on the dehydrogenation of propane*

The effect of CO_2 partial pressure on the dehydrogenation of propane over supported gallium oxide catalysts was also studied; the results are shown in Fig. 4. Propane conversion over Ga_2O_3/TiO_2 initially increased with the CO_2/C_3H_8 ratio, reaching its peak when the CO_2/C_3H_8 ratio equaled 2, then decreased with further increases in the CO_2/C_3H_8 ratio. In contrast, propane conversion over Ga_2O_3/Al_2O_3 and Ga_2O_3/ZrO_2 decreased continuously with increasing CO_2/C_3H_8 ratio, dramatically at the beginning and more slowly later on. In Ga_2O_3/MgO and Ga_2O_3/SiO_2, the increase in CO_2/C_3H_8 ratio had only a limited negative effect on propane conversion at first.

3.4. *Pulse reaction*

To obtain more information on the dehydrogenation of propane over various supported gallium oxide catalysts, CO_2 and H_2 pulse reaction, as well as CO_2 pulse reaction, were carried out. The results of the CO_2 and H_2 pulse reaction are shown in Fig. 5. The process is the reverse water–gas shift reaction, as shown in reaction (1). As shown in the figure, all of the supported gallium oxide catalysts except Ga_2O_3/SiO_2 displayed high activity for the reverse water–gas shift reaction,

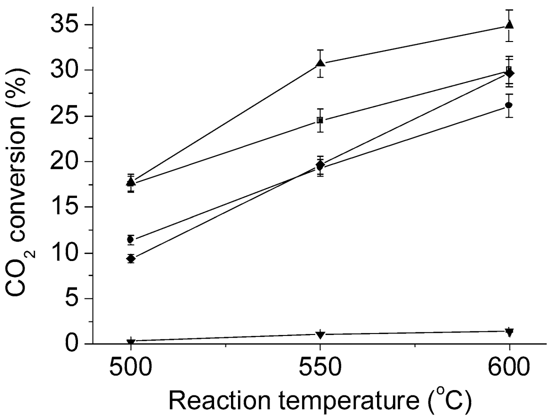

Fig. 5. Reaction data of CO_2 and H_2 pulse reaction: (■) Ga_2O_3/TiO_2; (●) Ga_2O_3/Al_2O_3; (▲) Ga_2O_3/ZrO_2; (▼) Ga_2O_3/SiO_2; (◆) Ga_2O_3/MgO.

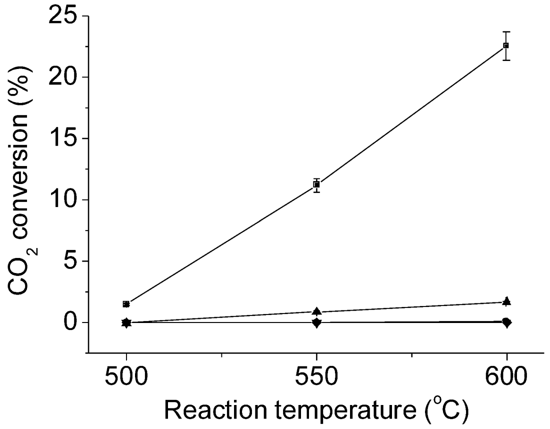

Fig. 6. Reaction data of CO_2 pulse reaction: (■) Ga_2O_3/TiO_2; (●) Ga_2O_3/Al_2O_3; (▲) Ga_2O_3/ZrO_2; (▼) Ga_2O_3/SiO_2; (◆) Ga_2O_3/MgO.

with activity increasing with increasing reaction temperature for all catalysts. At 600 °C, the extent of activity followed the order $Ga_2O_3/ZrO_2 > Ga_2O_3/TiO_2 \approx Ga_2O_3/MgO > Ga_2O_3/Al_2O_3 \gg Ga_2O_3/SiO_2$.

The reverse water–gas shift reaction can proceed only when both H_2 and CO_2 are adsorbed on the catalyst surface, as reported previously [22]. Purportedly, H_2 can be dissociatively adsorbed on gallium oxide and supported gallium oxide [20,23]; meanwhile, basic sites are also needed to adsorb CO_2. Therefore, the low activity of the reverse water–gas shift reaction over Ga_2O_3/SiO_2 can be attributed to its small amount of basic sites (Table 2).

CO_2 pulse reaction was also applied for further research. The results are illustrated in Fig. 6. When the supported gallium oxide catalyst was pretreated with H_2 for 30 min, a certain amount of H_2 was heterolytically dissociatively adsorbed on the catalyst surface [24], with the rate constant of k_1 as shown in reaction (3). Then the catalyst was treated with He for 10 min to remove H_2 in the reaction system. (That a certain amount of the chemisorbed H_2 desorbed simultaneously from the catalyst surface via the reverse reaction with the rate constant of k_2 was unavoidable, however.) Finally, a sufficient pulse of CO_2 was injected to react with H_2 remaining on the catalyst surface, with the rate constant of k_3:

$$\mathrm{Ga}^{x+}\text{–}\mathrm{O}^{2-}\text{–}\mathrm{M}^{y+} + \mathrm{H}_2 \underset{k_2}{\overset{k_1}{\rightleftharpoons}} \overset{\mathrm{H}^-}{\overset{|}{\mathrm{Ga}}}{}^{x+}\text{–}\overset{\mathrm{H}^+}{\overset{|}{\mathrm{O}}}{}^{2-}\text{–}\mathrm{M}^{y+} \xrightarrow[k_3]{\mathrm{CO}_2} \mathrm{Ga}^{x+}\text{–}\mathrm{O}^{2-}\text{–}\mathrm{M}^{y+} + \mathrm{CO} + \mathrm{H}_2\mathrm{O}$$

(M = Ga, Ti, Al, Zr, Si, or Mg). (3)

Because Ga_2O_3/ZrO_2, Ga_2O_3/TiO_2, Ga_2O_3/Al_2O_3, and Ga_2O_3/MgO are good catalysts for the reverse water–gas shift reaction, and because the amount of CO_2 injected is much larger than that of adsorbed H_2, the amount of CO produced through reaction (3) should connect directly with the amount of adsorbed H_2 remaining after purging with He for 10 min. The more CO produced, the more adsorbed H_2 remaining, and hence the smaller the k_2. Therefore, the CO_2 pulse reaction results suggest that the k_2 of Ga_2O_3/TiO_2 is much smaller than that of Ga_2O_3/ZrO_2, Ga_2O_3/Al_2O_3, and Ga_2O_3/MgO.

Table 7
Amount of H_2 chemisorbed on the supported gallium oxide catalysts (300 °C)

Catalyst	Amount of H_2 chemisorbed (μmol/g)
Ga_2O_3/TiO_2	2.4
Ga_2O_3/Al_2O_3	0.2
Ga_2O_3/ZrO_2	0.1
Ga_2O_3/SiO_2	0.2
Ga_2O_3/MgO	0.2

Table 8
Amount of propane chemisorbed in the absence and presence of CO_2 (300 °C)

Catalyst	Amount in the absence of CO_2 (μmol/g)	Amount in the presence of CO_2 (μmol/g)	Decreasing ratio (%)[a]
Ga_2O_3/TiO_2	4.2	2.5	40
Ga_2O_3/Al_2O_3	5.3	3.7	30
Ga_2O_3/ZrO_2	8.1	5.9	27
Ga_2O_3/SiO_2	1.1	1.1	0
Ga_2O_3/MgO	2.0	1.5	25

[a] Decreasing ratio = (1 − amount in the presence of CO_2)/(amount in the absence of CO_2) × 100%.

3.5. H_2 and propane chemisorption test

To gain more information on the role of CO_2 in the dehydrogenation reaction, the H_2 and propane chemisorption capacity of the supported gallium oxide catalysts was measured; the results are given in Tables 7 and 8. The tables show that at 300 °C, the H_2 chemisorption capacity of Ga_2O_3/TiO_2 was much higher than that of the other four catalysts, indicating that the chemisorbed H_2 over Ga_2O_3/TiO_2 is more stable and difficult to desorb, in agreement with the results of the pulse reactions.

The special H_2 adsorption property of Ga_2O_3/TiO_2 reported earlier may be connected to the abundant reduced gallium atoms on the Ga_2O_3/TiO_2 surface (45%), because reduced gallium ions ($Ga^{\delta+}$ cations, $\delta < 2$) are thought to have higher dehydrogenation efficiency [25], and a gallium–hydrogen bond can be formed on these reduced gallium ions by heterolytic hydrogen dissociation and can be stabilized on the support surface [20]. Only a small fraction or even no reduced gallium species could be detected on the other four supported gallium oxide catalysts, leading to the rapid desorption of H_2 on the surface.

The results also show that the propane adsorption capacity decreased when CO_2 was introduced to all catalyst except Ga_2O_3/SiO_2, which had a very low adsorption capacity. This decrease may be due to displacement of adsorbed propane by the CO_2 introduced, because CO_2 is obviously much more acidic than propane and thus much more readily adsorbed on the basic catalyst sites. But on Ga_2O_3/SiO_2, only a very small number of basic sites were detected by CO_2-TPD, indicating the catalyst's weak CO_2 adsorption ability; therefore, adding CO_2 in the gas flow has hardly any effect on this catalyst's propane adsorption capacity.

4. Discussion

The dehydrogenation of propane or ethane over reducible metal oxide catalysts, such as chromium and iron oxides, in the presence of CO_2 has been suggested to follow a redox mechanism [26,27]. Propane is oxidized to propene with the simultaneous reduction of metal oxide (e.g., Fe_2O_3, Cr_2O_3), and subsequently the reduced metal oxide catalyst is reoxidized by CO_2. According to our experimental results, supported gallium oxide catalysts cannot be reduced under the reaction temperature, and thus the redox mechanism is probably inapplicable for this reaction. It has been suggested that propane can be heterolytically dissociatively adsorbed on gallium oxide, forming gallium hydride and gallium alkoxide species [24]; the same process may occur over supported gallium oxide catalysts, as follows:

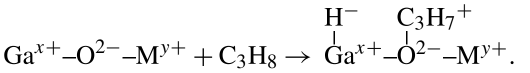

$$Ga^{x+}–O^{2-}–M^{y+} + C_3H_8 \rightarrow \overset{H^-}{Ga^{x+}}–\overset{C_3H_7^+}{O^{2-}}–M^{y+}. \quad (4)$$

The alkoxides further decompose to form the dehydrogenation products,

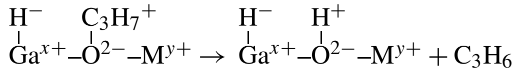

$$\overset{H^-}{Ga^{x+}}–\overset{C_3H_7^+}{O^{2-}}–M^{y+} \rightarrow \overset{H^-}{Ga^{x+}}–\overset{H^+}{O^{2-}}–M^{y+} + C_3H_6 \quad (5)$$

and

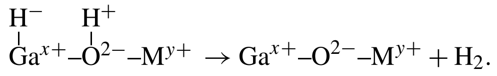

$$\overset{H^-}{Ga^{x+}}–\overset{H^+}{O^{2-}}–M^{y+} \rightarrow Ga^{x+}–O^{2-}–M^{y+} + H_2. \quad (6)$$

Step (5) is slow and represents the limiting step in propene formation [24]. When both Ga_2O_3 and H^+ are present on the catalyst, the propyl carbenium ion on Ga_2O_3 will readily exchange with a proton via a surface migration reaction [24],

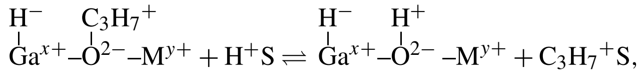

$$\overset{H^-}{Ga^{x+}}–\overset{C_3H_7^+}{O^{2-}}–M^{y+} + H^+S \rightleftharpoons \overset{H^-}{Ga^{x+}}–\overset{H^+}{O^{2-}}–M^{y+} + C_3H_7^+S, \quad (7)$$

in which S represents catalyst surface. Propene then results from the equilibrium,

$$C_3H_7^+S \rightleftharpoons C_3H_6 + H^+S. \quad (8)$$

The conjugated effect of gallium oxide and proton increases propane dehydrogenation activity by replacing the slow step (5) by the fast equilibria (7) and (8). Therefore, the amount of proton existing on the surface of the supported gallium oxide catalyst should have a considerable effect on the dehydrogenation activity.

The above reaction mechanism gives a good explanation for the different activities of the five supported gallium oxide catalysts toward the dehydrogenation reaction in the absence of CO_2, that is, the high activity of Ga_2O_3/ZrO_2, Ga_2O_3/TiO_2, and Ga_2O_3/Al_2O_3 and the low activity of Ga_2O_3/MgO and Ga_2O_3/SiO_2. NH_3-TPD studies showed that the medium to strong acid sites are more abundant on the surface of Ga_2O_3/ZrO_2, Ga_2O_3/TiO_2, and Ga_2O_3/Al_2O_3 than on Ga_2O_3/MgO and Ga_2O_3/SiO_2, which would facilitate the reactions (7) and (8) to bypass the slow step (5), thus enhancing the activity of propane dehydrogenation. The amount of medium to strong acid sites has the order $Ga_2O_3/ZrO_2 > Ga_2O_3/Al_2O_3 > Ga_2O_3/TiO_2 > Ga_2O_3/SiO_2 > Ga_2O_3/MgO$ (Table 1), exactly the same order as for the initial activity.

When CO_2 is introduced into the propane dehydrogenation reaction, chemisorbed H_2 formed from steps (5) and (7) can also be removed via an alternative route (9) (i.e., the reverse water–gas shift reaction), besides step (6):

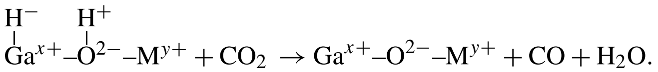

$$\overset{H^-}{Ga^{x+}}–\overset{H^+}{O^{2-}}–M^{y+} + CO_2 \rightarrow Ga^{x+}–O^{2-}–M^{y+} + CO + H_2O. \quad (9)$$

In fact, the major pathway of the removal of the dissociatively adsorbed H_2 depends on the relative rate of steps (6) and (9). Our pulse reaction tests and H_2 chemisorption measurements indicate that step (6) is relatively slow over Ga_2O_3/TiO_2. Therefore, the fast step (9) becomes the preferred reaction instead of the slow step (6) after CO_2 is introduced, because Ga_2O_3/TiO_2 has proven to be a good catalyst for the reverse water–gas shift reaction, which transforms H_2 with CO_2 into CO and H_2O, shifting the reactions (5) and (7) to the product side and thus enhancing the total reaction rate. In contrast, step (6) is relatively fast over Ga_2O_3/Al_2O_3, Ga_2O_3/ZrO_2, and Ga_2O_3/MgO and thus will still be the dominant reaction pathway for the removal of chemisorbed H_2 after introduction of CO_2. Thus, the enhancement effect of CO_2 on the total reaction rate is not evident for these catalysts. This can be further proven by the fact that the amount of CO_2 reacted on Ga_2O_3/TiO_2 via reaction (9) ($2 \times 20\%$) is close to the conversion of propane (32%) in the initial state (because the molar ratio of CO_2/C_3H_8 equals 2), whereas for Ga_2O_3/Al_2O_3, Ga_2O_3/ZrO_2, and Ga_2O_3/MgO catalysts, the amount of CO_2 participating in the reverse water–gas shift (9) is much lower than the conversion of propane (Tables 5 and 6). For Ga_2O_3/SiO_2, because activity for the reverse water–gas shift reaction is very low, it would be difficult for CO_2 to react with the chemisorbed H_2 over Ga_2O_3/SiO_2, and thus a positive effect of CO_2 would not be observed.

Meanwhile, CO_2 has a negative effect on the reaction by displacing the propane adsorbed on the catalyst surface [4,11]. Propane is dissociatively adsorbed on gallium oxide; basic sites are needed for the adsorption of $C_3H_7^+$, and acidic sites are needed for the adsorption of H^-. Because CO_2 is much more acidic than propane, the adsorption of CO_2 on the basic sites would certainly reduce the possibility of the adsorption of propane on gallium oxide, leading to reduced propane conversion. This phenomenon is demonstrated by the greatly reduced adsorption capacity of propane over most supported catalysts after the introduction of CO_2 (Table 8). For those catalysts with activity enhanced by the addition of CO_2, such as Ga_2O_3/TiO_2, the negative effect of CO_2 displacement on the reaction is not as evident at a low concentration of CO_2, and propane conversion increases with increasing CO_2/C_3H_8 ratio. When the CO_2 concentration increases, this negative effect becomes dominant, and the propane conversion begins to decrease. For such catalysts as Ga_2O_3/Al_2O_3 and Ga_2O_3/ZrO_2, the addition of CO_2 does not have a promoting effect on activity, the negative effect of CO_2 will always prevail. This explains why the propane conversion over Ga_2O_3/TiO_2 has a maximum with increasing CO_2/C_3H_8 ratio, whereas the conversion over Ga_2O_3/Al_2O_3 and Ga_2O_3/ZrO_2 decreases continuously from the very beginning with increasing CO_2/C_3H_8 ratio (Fig. 4). For Ga_2O_3/SiO_2 and Ga_2O_3/MgO, the rate-determining step (reaction (5)) is very slow, because there are insufficient protons to exchange with $C_3H_7^+$ via reaction (7) to circumvent this slow reaction. Therefore, the decreased rate of reaction (4) by the displacement of CO_2 against propane would have only a limited negative effect on the rate-limiting step (5) (Fig. 4).

5. Conclusion

Dehydrogenation of propane to propene in the absence or presence of CO_2 over five supported gallium oxide catalysts was investigated, and distinct behaviors were observed. Ga_2O_3/TiO_2, Ga_2O_3/Al_2O_3, and Ga_2O_3/ZrO_2 are better catalysts for the dehydrogenation reaction than Ga_2O_3/SiO_2 and Ga_2O_3/MgO, because they contain many more acid sites of medium to strong and strong strength on the surface. CO_2 has a promoting effect on dehydrogenation activity over Ga_2O_3/TiO_2 but a negative effect over Ga_2O_3/ZrO_2 and Ga_2O_3/Al_2O_3. These different support effects may derive from the catalysts' differing H_2 adsorption capacities and acid–base properties, probably caused by the differing interactions between the gallium oxide and the support. XPS studies showed abundant reduced gallium atoms (45%) on the surface of Ga_2O_3/TiO_2, which may account for this catalyst's unique catalytic behavior in the dehydrogenation reaction in the presence of CO_2. Results for the pulse reaction and dehydrogenation reaction with varying partial pressures of CO_2 indicate that CO_2 plays two roles in the dehydrogenation reaction: a positive role by removing absorbed H_2 on the catalyst surface through the reverse water–gas shift reaction and a negative role by displacing propane adsorbed on the catalyst's basic sites. Dehydrogenation proceeds on the supported gallium oxide catalysts probably through a heterolytic dissociation reaction pathway instead of a redox mechanism, similar to that on pure gallium oxide.

Acknowledgments

This work was supported by the Chinese Major State Basic Research Development Program (grant 2000077507), the National Natural Science Foundation of China (grant 20303004), the Shanghai Major Basic Research Program (grant 03DJ14004), and the Shanghai Natural Science Foundation (grant 03ZR14013).

References

[1] I. Takahara, M. Saito, Chem. Lett. (1996) 973.
[2] I. Takahara, W.C. Chang, N. Mimura, M. Saito, Catal. Today 45 (1998) 55.
[3] B. Zhaorigetu, R. Kieffer, J.P. Hindermann, Stud. Surf. Sci. Catal. 101 (1996) 1049.
[4] K. Nakagawa, M. Okamura, N. Ikenaga, T. Suzuki, T. Kobayashi, Chem. Commun. (1998) 1025.
[5] P. Meriaudeau, C. Naccache, J. Mol. Catal. 50 (1989) L7.
[6] P. Schulz, M. Baerns, Appl. Catal. 78 (1991) 15.
[7] M. Guisnet, N.S. Gnep, F. Alario, Appl. Catal. A 89 (1992) 1.
[8] Y. Ono, Catal. Rev. Sci. Eng. 34 (1992) 179.
[9] B.S. Kwak, W.M.H. Sachtler, J. Catal. 145 (1994) 456.
[10] P. Meriaudeau, C. Naccache, Catal. Today 31 (1996) 265.
[11] K. Nakagawa, C. Kajita, Y. Ide, M. Okamura, S. Kato, H. Kasuya, N. Ikenaga, T. Kobayashi, T. Suzuki, Catal. Lett. 64 (2000) 215.
[12] K. Nakagawa, C. Kajita, K. Okumura, N. Ikenaga, M. Nishitani-Gamo, T. Ando, T. Kobayashi, T. Suzuki, J. Catal. 203 (2001) 87.
[13] P. Michorczyk, J. Ogonowski, Appl. Catal. A 251 (2003) 425.
[14] P. Michorczyk, J. Ogonowski, React. Kinet. Catal. Lett. 78 (2003) 41.
[15] M. Saito, S. Watanabe, I. Takahara, M. Inaba, K. Murata, Catal. Lett. 89 (2003) 213.
[16] B. Zheng, W.M. Hua, Y.H. Yue, Z. Gao, J. Catal. 232 (2005) 143.
[17] R. Carli, C.L. Bianchi, R. Giannantonio, V. Ragaini, J. Mol. Catal. 83 (1993) 379.
[18] V. Parvulescu, S. Coman, V.I. Parvulescu, P. Grange, G. Poncelet, J. Catal. 180 (1998) 66.
[19] M. Haneda, Y. Kintaishi, H. Shimada, H. Hamada, Chem. Lett. (1998) 181.
[20] S.E. Collins, M.A. Baltanas, J.L.G. Fierro, A.L. Bonivardi, J. Catal. 211 (2002) 252.
[21] B.M. Reddy, I. Ganesh, E.P. Reddy, A. Fernandez, P.G. Smirniotis, J. Phys. Chem. B 105 (2001) 6227.
[22] C.S. Chen, W.H. Cheng, S.S. Lin, Appl. Catal. A 238 (2003) 55.
[23] S.E. Collins, M.A. Baltanas, A.L. Bonivardi, Langmuir 21 (2005) 962.
[24] P. Meriaudeau, C. Naccache, J. Mol. Catal. 59 (1990) L31.
[25] I. Nowak, J. Quartararo, E.G. Derouane, J.C. Védrine, Appl. Catal. A 251 (2003) 107.
[26] S.B. Wang, K. Murata, T. Hayakawa, S. Hamakawa, K. Suzuki, Appl. Catal. A 196 (1998) 1.
[27] P. Michorczyk, P. Kustrowski, L. Chmielarz, J. Ogonowski, React. Kinet. Catal. Lett. 82 (2004) 121.